Bioorganic & Medicinal Chemistry Letters 21 (2011) 3596–3602

Contents lists available at ScienceDirect

Bioorganic & Medicinal Chemistry Letters

journal homepage: www.elsevier.com/locate/bmcl

Discovery of a potent and selective small molecule hGPR91 antagonist

Debnath Bhuniya [a,*], Dhananjay Umrani [a], Bhavesh Dave [a], Deepak Salunke [a], Gagan Kukreja [a], Jayasagar Gundu [a], Minakshi Naykodi [a], Nadim S. Shaikh [a], Prasad Shitole [a], Santosh Kurhade [a], Siddhartha De [a], Sreemita Majumdar [a], Srinivasa B. Reddy [a], Suhas Tambe [a], Yogesh Shejul [a], Anita Chugh [a], Venkata P. Palle [a], Kasim A. Mookhtiar [a], Doris Cully [b], Joseph Vacca [b], Prasun K. Chakravarty [b], Ravi P. Nargund [b], Samuel D. Wright [b], Michael P. Graziano [b], Sheo B. Singh [b], Sophie Roy [b], Tian-Quan Cai [b]

[a] Drug Discovery Facility, Advinus Therapeutics, Quantum Towers, Plot-9, Phase-I, Rajiv Gandhi InfoTech Park, Hinjewadi, Pune 411 057, India
[b] Merck Research Laboratories, PO Box 2000, Rahway, NJ 07065, USA

ARTICLE INFO

Article history:
Received 17 March 2011
Revised 18 April 2011
Accepted 22 April 2011
Available online 28 April 2011

Keywords:
GPR91
Succinate
hGPR91 antagonist
Structure–activity relationship
Pharmacodynamic effect

ABSTRACT

GPR91, a 7TM G-Protein-Coupled Receptor, has been recently deorphanized with succinic acid as its endogenous ligand. Current literature indicates that GPR91 plays role in various pathophysiology including renal hypertension, autoimmune disease and retinal angiogenesis. Starting from a small molecule high-throughput screening hit **1** (hGPR91 IC_{50}: 0.8 μM)—originally synthesized in Merck for Bradykinin B_1 Receptor (BK_1R) program, systematic structure-activity relationship study led us to discover potent and selective hGPR91 antagonists e.g. **2c**, **4c**, and **5g** (IC_{50}: 7–35 nM; >1000 fold selective against hGPR99, a closest related GPCR; >100 fold selective in Drug Matrix screening). This initial work also led to identification of two structurally distinct and orally bio-available lead compounds: **5g** (%F: 26) and **7e** (IC_{50}: 180 nM; >100 fold selective against hGPR99; %F: 87). A rat pharmacodynamic assay was developed to characterize the antagonists in vivo using succinate induced increase in blood pressure. Using two representative antagonists, **2c** and **4c**, the GPR91 target engagement was subsequently demonstrated using the designed pharmacodynamic assay.

Succinate, a Kreb's cycle intermediate, has been recently characterized by He et al. as an endogenous ligand of GPR91, a 7TM G-Protein-Coupled Receptor (GPCR) and a novel target for drug discovery.[1] The closest protein related to GPR91 is another 7TM GPCR called GPR99 sharing 33% protein sequence identity. GPR99 has also been deorphanized with another tricarboxylic acid (TCA) cycle intermediate, α-ketoglutarate, by the same research group.[1] Whereas, succinate activates GPR91 through both G_i and G_q mediated signaling pathways (EC_{50} $[Ca^{2+}]_i$: 28–56 μM in HEK293 cells stably expressing hGPR91), α-ketoglutarate seems to act exclusively via G_q signaling (EC_{50} $[Ca^{2+}]_i$: 32–69 μM).[1,2] Interestingly, these two receptors also have distinctions in their expression pattern in various tissues. Whereas, GPR91 has been shown to express in tissues like kidney, liver, adipose, spleen, heart, retina and intestine, GPR99 is largely expressed in kidney, smooth muscle and testis.[1,3–5]

Role of Succinate in hypertension, at least in animals, has been demonstrated through several in vivo and in vitro mechanistic studies.[1,6–8] Succinate treatment leads to increase in mean arterial pressure (MAP) via GPR91 mediated action on plasma rennin activity and subsequent activation of renin-angiotensin system (RAS).[1] Succinate is accumulated in extra-cellular spaces under hyperglycemic or ischemic condition. It has been hypothesized that such an ischemic condition may lead to manifestation of mitochondrial dysfunction and the release of succinate as a signal to activate GPR91 to regulate local blood flow in order to match metabolic demands.[6,8] Therefore, antagonists of the receptor may prove helpful in reversing pathophysiology under the clinical setting of renal hypertension and diabetic nephropathy.

In addition, independent works from various research groups have indicated other potential therapeutic implication of GPR91 antagonism.[9–11] GPR91 is highly expressed in quiescent hepatic stellate cells (HSC)[9] and spleen dendritic cells (DCs).[10] In DCs, succinate induced agonism of GPR91 lead to production of proinflammatory cytokines. Succinate induced signaling through GPR91 in liver stellate cells as well as in spleen dendritic cells could lead to antigen-driven responses of T-cells which correlates to inflammation and autoimmune diseases.[9,10] Function of succinate and GPR91 (present in retinal ganglion neurons) have also been described in establishing neovascular network during retinal angiogenesis and in response to injury.[5,11]

Despite a rapid advancement of GPR91 biology, pharmacological validation of the target could not been achieved mainly due

* Corresponding author. Tel.: +91 20 66539600; fax: +91 20 66539620.
E-mail address: debnath.b@advinus.com (D. Bhuniya).

0960-894X/$ - see front matter © 2011 Elsevier Ltd. All rights reserved.
doi:10.1016/j.bmcl.2011.04.091

to the fact that GPR91 antagonists were not available as tool compounds.[12] We report herein identification of the first potent and selective small molecule GPR91 antagonists towards unfolding therapeutic potential of the target.

From a high-throughput screening of internal sample collection at Merck, using hGPR91 over-expressed CHO-K1 stable cell-line, **1** (Fig. 1) was identified as a hit (IC_{50} of 0.8 μM with complete inhibition of succinate induced increase in intra-cellular Ca^{2+} pool) which served as a starting point for hit-to-lead identification.[13] The hit **1** was originally synthesized and evaluated for Bradykinin B_1 Receptor (BK_1R) inhibitory activity at Merck. The modest BK_1R activity associated with **1** (IC_{50}: 2.5 μM) was expected to be dialed out during the drug optimization simply by removal of carboxylic ester present in its biphenyl part.[14] To drive medicinal chemistry around the hit **1**, the structure–activity relationship (SAR) studies were divided into three categories: (a) around the biphenyl tail, (b) the propylene-carbonyl linker, (c) and the naphthyridin-2-yl head (Fig. 1). SAR exercise to optimize the tail part provided us a major break through, whereas a little variation of naphthyridine part was found to be too intolerant to develop any SAR. Key findings of initial SAR work, carried out with the linker and tail parts, are summarized in this communication.

In one of the early investigation of SAR, we noticed that the hit **1** lost its hGPR91 activity upon changing its methyl carboxylate into the corresponding acid **2a**. However, we were inspired to see that the unsubstituted biphenyl compound **2b** was almost equipotent to the hit **1**. Additionally, the BK_1R activity was completely dialed out in **2b**. Hence **2b** (IC_{50}: 1 μM; metabolic clearance in rat liver microsome CL: 0.17 nmol/min/mg RLM) was considered as a more tractable hit for SAR development for what the initial goal was to improve hGPR91 potency while maintaining the metabolic stability **(**for SAR summary, see Fig. 1, **I-1)**. We found that *meta* position of the terminal phenyl ring (termed as R^3) in **2b** was very responsive for developing a SAR. Small hydrophobic substitutions like –Me, –Cl, $–CF_3$ (examples **2c**–**e**), among the several sterically and electronically tuned substitutions tested, significantly improved the potency often by 30 fold. Though the smallest substitution (e.g., –F) at the *para* position (termed as R^4) maintained the potency, any larger substitution at that position led to loss of activity (compare data of **2c** & **2e** vs **2u**). The *m*-CF_3 (R^3) and *p*-F (R^4) substituted compound **2e** was considered as an optimized compound (IC_{50}: 22 nM and CL: 0.1 nmol/min/mg RLM) from the early SAR study. Further improvement in hGPR91 potency was achieved in **2j** (~3 fold compared to **2d**) by addition of a methyl group at benzylic carbon (termed as R^5) however without any improvement of metabolic stability. For further SAR information on biphenyl tail part (**I-1**), Table S1 of Supplementary data is referred.

Next set of SAR iteration was planned on propylene linker in **2b** with an intension of arresting a possible CYP mediated metabolism at the aliphatic chain (Fig. 1, **I-2**; see Supplementary data Table S2 for preliminary SAR information). Upon constraining the propylene linker with *para*-phenylene moiety indeed resulted in metabolically very stable compound **3** (CL: 0.02 nmol/min/mg RLM) but completely lost hGPR91 activity. We rationalized that the phenylene–cabonyl moiety might have destroyed the required flexibility in the linker region. Therefore, a methylene linker was introduced between the phenylene and cabonyl group which in combination with the most prefered tail part ($R^3 = CF_3$, $R^4 = F$, $R^5 = (S)$-Me)

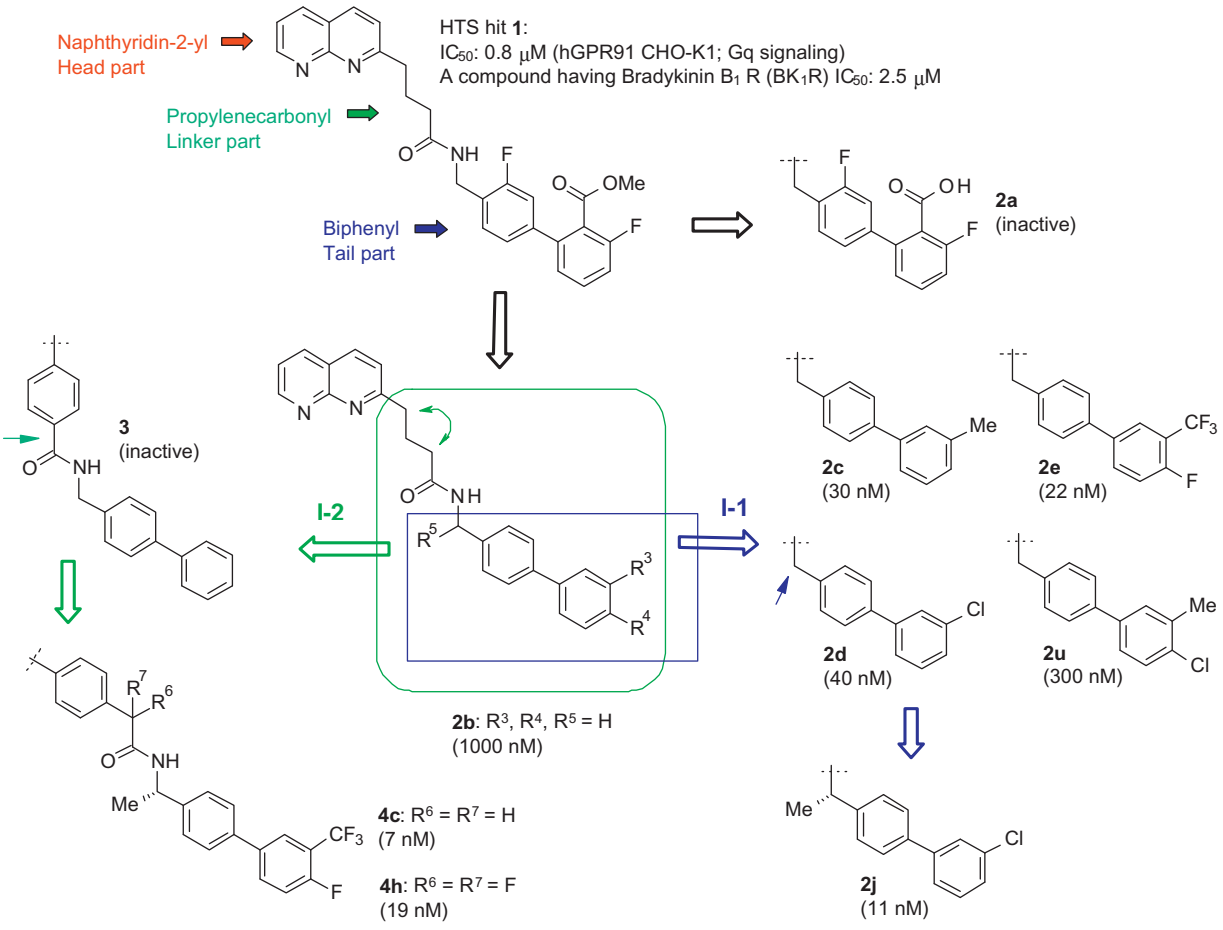

Figure 1. Structure of HTS hit **1** and the initial SAR summary (the tail and linker parts).

resulted in potent and stable compound **4c** (IC_{50}: 7 nM; CL: 0.2 nmol/min/mg RLM). Substitution like –Me, –F, $–CF_3$, –OH, $–NH_2$ were also attempted at α-C of amide functionality (R^6 & R^7) to follow the effect on hGPR91 potency as well as impact on metabolic stability. Except for the case of $-NH_2$ (e.g., **4f**), the hGPR91 potency was more or less maintained in these analogs (e.g. **4d**–**e**, **4g**–**j**) in addition to retention of metabolic stability. Antagonists **4c** and **4h** (IC_{50}: 19 nM, CL: 0.14 nmol/min/mg RLM) were considered as optimized compounds from that particular SAR work.

At that stage of the program, we considered few potent hGPR91 antagonists which were selective against hGPR99 for pharmacokinetic (PK) evaluation before embarking on pharmacodynamic (PD) or in vivo target engagement studies. Unfortunately, lead compounds from series 2 and 4 did not offer satisfactory oral bioavailability (tested in Wistar rats) although some of them exhibited low plasma clearance reflecting the metabolic stability seen in RLM. None the less, reasonable plasma exposure was achieved upon administration of these compounds via intra-peretonial (i.p.) route. In vitro and PK profile of representative leads **2c**, **2d**, **2j** and **4c** are summarized in Table 1.

Needless to mention here that there was a strong need to improve oral bioavailability of lead compounds from the series 2 and 4 for the purpose of their robust utility as pharmacological tool. Therefore our next round of optimization was focused on balancing hGPR91 potency, selectivity against hGPR99, metabolic stability and oral bioavailability. The SAR efforts along this direction are summarized in Figure 2 (**I-3** and **I-4**). Further SAR data are presented in Supplementary data Tables S3 and S4.

We envisaged that the penultimate phenylene ring in the biphenyl tail part of 2e could be considered as next point of SAR (I-3) where the aromatic ring would be replaced with a heteroaromatic ring. As presented in Table S3 nine heteroarylene moieties (H1–H9), tethered to the most optimimally substituted terminal phenyl ring ($R^3 = CF_3$, $R^4 = F$), were considered for SAR investigation. We were delighted to notice that the pyrimidin-2,5-ylene (H1) and isoxazol-3,5-ylene (H5) analogs **5a** and **5g** respectively could retain the potency with satisfactory metabolic stability (IC_{50}: 49, 35 nM; CL: 0.2, 0.12 nmol/min/mg RLM respectively). It was interesting to note a 4 fold difference in potency between the two differently connected pyrimidines H1 and H2 (e.g. **5a** vs **5b**). Among the others, pyrazole analog **5d** also exhibited good potency and stability (IC_{50}: 210 nM; CL: 0.18 nmol/min/mg RLM). From this optimization study, **5g** was identified as next improved compound having demonstrated satisfactory oral bioavailability in rats (%F: 26; vehicle: supension in 0.5% CMC), very good plasma concentration (C_{max}: 37 μM and $AUC_{0-24\ h}$: 69 μM h at 30 mg/kg p.o. dose), and low plasma clearance (4.7 mL/min/kg). In addition, **5g** was found to be selective against hGPR99 and a pannel of >120 off-targets (see Table 1). It is important to note here that going from **2e** to **5g**, *c* Log *P* value reduced from 4.87 to 3.56 resulting in improvement of oral bioavailability.

In another SAR exercise, effect of bio-isosteric replacement of amide functionality was studied in structure **2** (Fig. 2, **I-4**; Table S4). Out of three isosteric heterocycles H8-10 tested, 1,3,4-oxadiazol-2,5-ylene H8 was found to be superior over the other two in retaining hGPR91 activity. The compound **6a** ($R^3 = Cl$) was a potent hGPR91 antagonist (IC_{50}: 40 nM) and selective against hGPR99 (IC_{50}: >30 μM). However, **6a** (*c* Log *P*: 5.34) did not offer us adequate oral bioavailability; hence it was considered for further optimization to improve its drug-like properties by reducing its lipophylicity. It was envisaged that the biphenyl-oxadiazole part in **6a** might be made less hydrophobic by curtailing one phenyl group. Accordingly, the linker length was increased by a bond to compensate the length of the designed molecule, and another round of SAR iteration was carried out on substitutions in the terminal ring (R^3 & R^4 of **7** in Table S4). Compound **7d**–**f** ($R^3 = CF_3$, Cl, CF_3; $R^4 = CF_3$, OCF_3, Cl respectively) were found to have satisfactory hGPR91 potency (160–180 nM) and metabolic stability (CL: 0.17–0.3 nmol/min/mg RLM). Once again, a *meta*-substitution (R^3) was found to improve the hGPR91 potency (**7b**–**c** vs **7d**–**f**). Interestingly, unlike in series **2**, larger substitutions like Cl, CF_3, OCF_3 at *para*-position (R^4) of the terminal phenyl ring was preferred in this series (**7d**–**f** vs **7g**) presumably because of shorter length of these compounds compared to series **2**–**5**. In vitro and PK data of representative leads **7e** ($R^3 = Cl$; $R^4 = OCF_3$) and **7f** ($R^3 = CF_3$; $R^4 = Cl$) are presented in Table 1 which clearly indicate that these compounds are selective against hGPR99, and have the desirable PK characteristics. As for example, **7e** (*c* Log *P*: 4.53) demonstrated low plasma

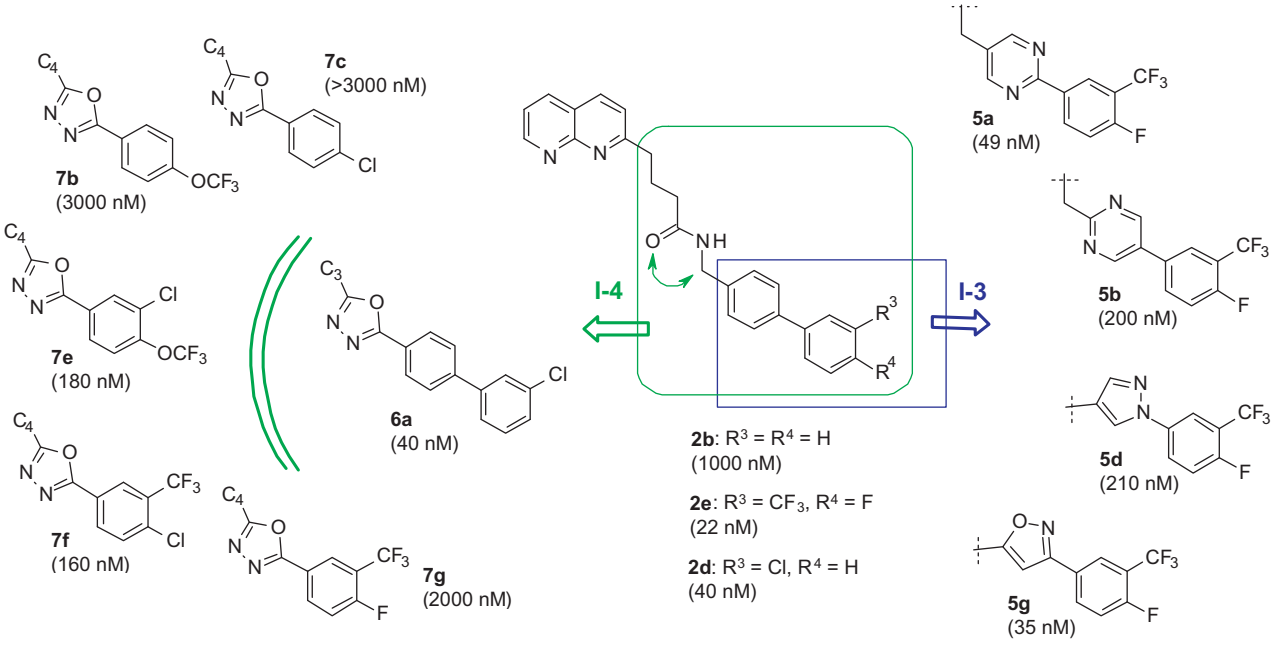

Figure 2. SAR summary to identify leads with desirable oral PK properties.

Table 1
In vitro and PK profile of selected compounds

Antagonists	hGPR91[a] IC_{50} (nM)	rGPR91[a] IC_{50} (nM)	hGPR99[a] IC_{50} (μM)	CL[b] (nmol/min/mg)	Rat PK[c]
2c[d]	30 ± 2 (n = 14)	7 ± 3 (n = 4)	>30	1.2	i.v. (5 mg/kg): C_{max} 19 ± 1.4 μM; CL 64.7 ± 9 mL/min/kg; V_{ss} 0.5 ± 0.0 L/kg; $t_{1/2}$ 0.1 ± 0.01 h. i.p. (50 mg/kg): C_{max} 3.7 ± 1.6 μM; T_{max} 1.8 ± 0.3 h; $AUC_{0-8\ h}$ 17.4 ± 2.3 μM h; $C_{2\ h}$ 3.3 ± 0.8 μM; $C_{4\ h}$ 2.4 ± 0.3 μM; $C_{8\ h}$ 1.1 ± 0.3 μM.
2d	40 ± 9	115 ± 25	7 ± 2	0.3	i.v. (5 mg/kg): C_{max} 82.7 ± 10.4 μM; CL 4.4 ± 0.6 mL/min/kg; V_{ss} 0.2 ± 0.05 L/kg; $t_{1/2}$ 1.2 ± 0.3 h. i.p. (50 mg/kg): C_{max} 17.8 ± 4.3 μM; T_{max} 3.3 ± 1.2 h; $AUC_{0-8\ h}$ 119 ± 29 μM h; $C_{8\ h}$ 15 ± 5 μM.
2j	11 ± 1	100 ± 15	2 ± 0.6	0.42	i.v. (5 mg/kg): C_{max} 19 ± 4 μM; CL 14.8 ± 0.6 mL/min/kg; V_{ss} 0.7 ± 0.1 L/kg; $t_{1/2}$ 0.8 ± 0.2 h.
4c[d]	7 ± 2 (n = 5)	—[e]	>30	0.2	i.v. (3 mg/kg): C_{max} 9.8 ± 4 μM; CL 36 ± 5.0 mL/min/kg; V_{ss} 1.0 ± 0.2 L/kg; $t_{1/2}$ 0.9 ± 0.2 h. i.p. (100 mg/kg): C_{max} 0.4 ± 0.1 μM; T_{max} 4.9 ± 3 h; $AUC_{0-24\ h}$ 4.3 ± 3.2 μM h; $C_{2\ h}$ 0.24 ± 0.08 μM; $C_{4\ h}$ 0.33 ± 0.1 μM; $C_{8\ h}$ 0.28 ± 0.2 μM.
5g[d]	35 ± 3 (n = 5)	135 ± 63	>30	0.12	i.v. (5 mg/kg): C_{max} 40 ± 3 μM; CL 4.7 ± 2.1 mL/min/kg; V_{ss} 0.36 ± 0.1 L/kg; $t_{1/2}$ 1.1 ± 0.3 h. i.p. (50 mg/kg): C_{max} 22 ± 4 μM; T_{max} 2 ± 0.0 h; $AUC_{0-8\ h}$ 267 ± 40 μM h; $C_{2\ h}$ 22 ± 4 μM; $C_{4\ h}$ 19 ± 2 μM; $C_{8\ h}$ 19 ± 5 μM. p.o. (30 mg/kg): C_{max} 37 ± 4.5 μM; T_{max} 0.5 ± 0.0 h; $C_{2\ h}$ 11.3 ± 5.7 μM; $C_{4\ h}$ 2.6 ± 0.7 μM; $AUC_{0-24\ h}$ 69 ± 12 μM h; $t_{1/2}$ 0.9 ± 0.1 h; %F 26.
6a	40 ± 1	67 ± 5	5 ± 1	0.3	i.v. (5 mg/kg): C_{max} 9.3 ± 0.9 μM; CL 51 ± 3 mL/min/kg; V_{ss} 1.9 ± 0.9 L/kg; $t_{1/2}$ 0.9 ± 0.6 h.
7e	180 ± 28	—[e]	>20	0.17	i.v. (5 mg/kg): C_{max} 56 ± 6 μM; CL 2.0 ± 0.2 mL/min/kg; V_{ss} 0.2 ± 0.0 L/kg; $t_{1/2}$ 1.3 ± 0.2 h. p.o. (30 mg/kg): C_{max} 72 ± 2.8 μM; T_{max} 1.5 ± 0.8 h; $C_{2\ h}$ 70 ± 0.2 μM; $C_{4\ h}$ 40.5 ± 7.2 μM; $AUC_{0-24\ h}$ 471.5 ± 198 μM.h; $t_{1/2}$ 3.4 ± 2.0 h; %F 87.
7f	160 ± 0.0	435 ± 22	>30	0.3	i.v. (5 mg/kg): C_{max}: 92 ± 34 μM; CL: 4.8 ± 1.6 mL/min/kg; V_{ss}: 0.1 ± 0.03 L/kg; $t_{1/2}$: 0.3 ± 0.1 h. i.p. (50 mg/kg): C_{max} 21 ± 6 μM; T_{max} 2.7 ± 1.2 h; $AUC_{0-8\ h}$ 304 ± 91 μM h; $C_{2\ h}$ 19 ± 3 μM; $C_{4\ h}$ 20 ± 7 μM; $C_{8\ h}$ 15 ± 5 μM.

[a] A brief description of hGPR91, rGPR91, and hGPR99 assay development and screening protocol is available as supplementary material. Details will be reported in a separate communication. IC_{50} values are presented as average ± SD from at least two independent 9 point titration experiments. Data collections were done in triplicate.
[b] Measured as intrinsic metabolic clearance of tested drug (CL, nmol/min/mg of RLM). Based on our RLM metabolic stability assay protocol (see Supplementary data), a CL range of 0.1–0.3 was indicative of good stability; 0.4–0.6 as moderate stability.
[c] Vehicle information: (i) Solution prepared using DMAC (10–20%) + CrEL (10%) + PEG400 (10%) in saline or DMAC (10%) + ethanol (10%) + PG (10%) + MQ water (70%) for i.v. administration (5 mL/kg dose volume). (ii) Suspension prepared using CMC (0.5%) + Tween 80 (0.5%) in water for i.p. and oral dosing. PK parameters are presented as mean value of three animals ± SD. Supplementary data referred for detailed PK experiments.
[d] Demonstrated >100 fold selectivity against >120 off-targets (MDS PanLab).
[e] rGPR91 data not generated for these compounds. However, the data of their close analogs indicate for no species difference between rat and human.

clearance (2.0 mL/min/kg), excellent bioavailability (%F: 87) and drug exposure (C_{max}: 72 μM, $AUC_{0-24\ h}$: 471 μM h; $t_{1/2}$: 3.4 h) upon oral administration (30 mg/kg p.o.) in Wistar rats.

To study GPR91 target engagement in vivo, a pharmacodynamic (PD) assay was developed based on the initial report of He et al.[1] Details of the PD assay development and pharmacological characterization of GPR91 antagonists will be a subject matter of another report. In brief, bolus administration of succinate (1 mg/kg i.v.) to overnight fasted and anesthetized male Wistar rats led to a transient increase of mean arterial pressure (MAP). Rats exhibiting an increasing of MAP by at least 10 mm Hg above the saline-induced change in MAP, were considered for the PD study (ΔMAP >10 mm Hg as the PD window). A schematic diagram of the PD assay protocol is outlined in Figure 3.

To estimate the effect of GPR91 antagonists on succinate induced increase in MAP, two time points were considered at 2 and 4 h (SA2 and SA3) post-drug dose. An effect from a pre-drug dose time point SA1 was chosen as the study control. PD data of two representative antagonists **2c** and **4c** are presented here in

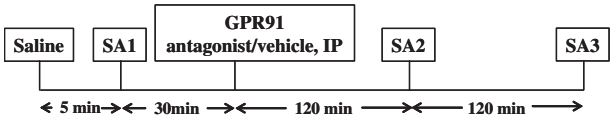

Figure 3. Protocol for the pharmacodynamic (PD) assay. Saline, SA1, SA2 and SA3: Vehicle and succinate doses (1 mg/kg i.v. bolus) followed by measurement of ΔMAP. The antagonistic effects are measured from percent inhibition of ΔMAP independently at SA2 and SA3 time points in comparison to the ΔMAP measured at SA1 time point.

Figure 4. Compounds were dosed i.p. which allowed us to do drug delivery when the animals were under anesthetized condition. In addition, i.p. dosing offered sustained drug exposure during the PD study. **2c** (50 mg/kg, i.p.) demonstrated 71 and 67% inhibition of succinate-induced rise in ΔMAP measured at 2 and 4 h (SA2 and SA3 time points) post drug dose. Plasma drug levels were found to be 1.8 and 2.0 μM respectively. Drug concentration in kidney was found to be 7.0 μM measured soon after SA3 time point. **4c**

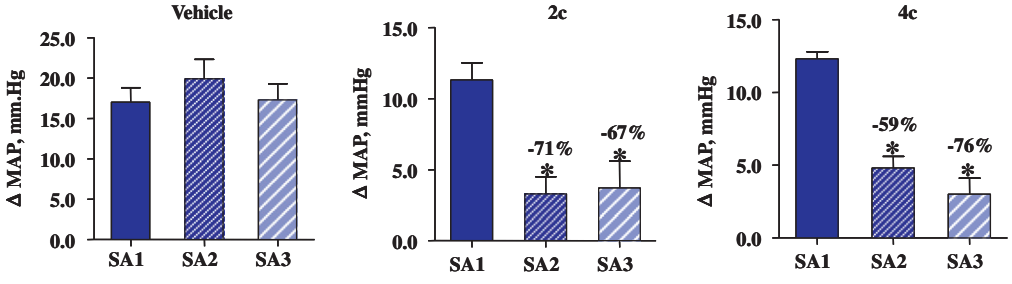

Figure 4. In vivo target engagement by the GPR91 antagonists **2c** and **4c** in the Pharmacodynamic (PD) assay. Data are shown as mean ± S.E.M. *Significantly different as compared to SA1. Unpaired t-test, p <0.05. Numbers above the bars indicate% inhibition of succinate (SA) induced increase in mean arterial pressure (ΔMAP) at that time point.

(100 mg/kg, i.p.) led to 59 and 76% inhibition of ΔMAP at 2 and 4 h (drug exposure: 0.2 & 0.3 μM in plasma; 8 μM in kidney). Both the compounds had shown rat plasma protein binding 99%. Considering their intrinsic rGPR91 potency in the range of 10–30 nM, the observed kidney exposure in the range of 7–8 μM can explain the PD effect. These preliminary results strongly suggest that these small molecule GPR91 antagonists indeed have engaged the target under the in vivo condition.

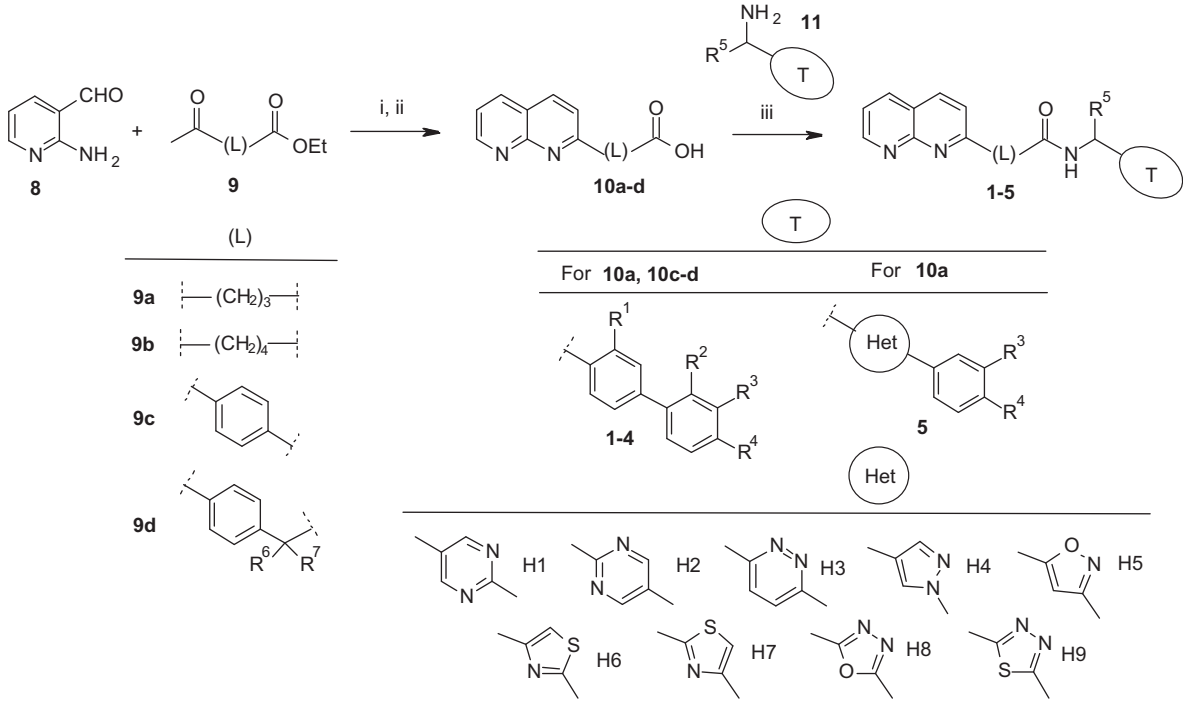

Scheme 1. General synthetic route to amide series of compounds **1**–**5**. Reaction condition: (i) L-Proline, EtOH, reflux, 20 h. 42–55%; (ii) LiOH·H_2O, THF, H_2O, rt, 16 h, 70–83%; (iii) EDCI, HOBt, NMM, DMF, rt, 18 h, 40–85%.

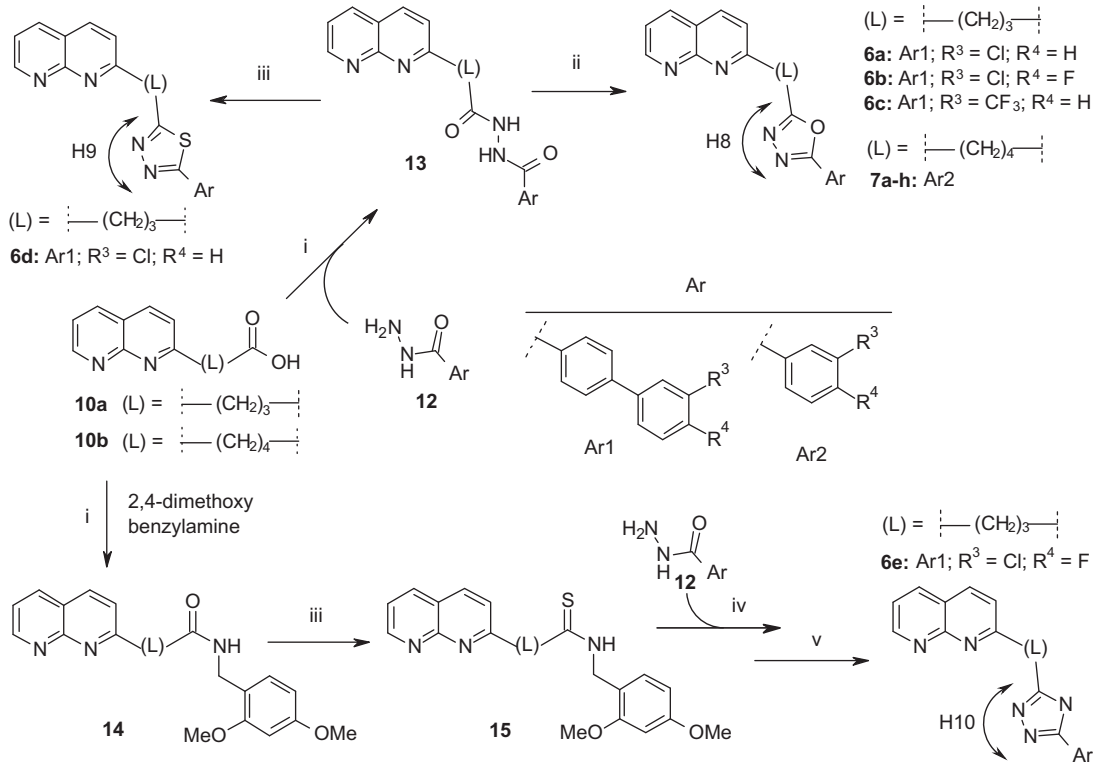

Scheme 2. General synthetic routes to amide bio-isosteric compounds **6**–**7**. Reaction condition: (i) EDCI, HOBt, NMM, DMF, rt, 18 h, 40–85%; (ii) $POCl_3$, ethylene dichloride, 100 °C, 3 h., 45%; (iii) Lawessons reagent, THF, reflux, 16 h, 99%; (iv) $Hg(OAc)_2$, THF, 0 °C, 2 h, 40%; (v) TFA, DCM, 0–rt, 18 h, 68%.

General and typical synthetic routes employed to access the GPR91 antagonists are outlined in Scheme 1 and Scheme 2. 1,8-Naphthyridine heterocycle was constructed having appropriate 2- substitution via Friedländer heterocyclization[15] between 2-amino-3-formylpyridine **8**[16] and appropriately chosen methylketoester **9**. Subsequent ester hydrolysis provided us the carboxylic acid **10** as a common building block for synthesis of both the amide (**1-5**) as well as amide bio-isosteric compounds (**6-7**).

The scaffold **10** was reacted with appropriately chosen amine **11** using EDCI/HOBt promoted amide coupling condition to obtain the antagonists **1**–**5** (Scheme 1).[17–19]

The acid intermediates **10a**–**b**, synthesized in Scheme 1, were used for the synthesis of amide bio-isosters **6** and **7** shown in Scheme 2. Starting from **10a**–**b**, and reacting with acylhydrazine **12**, another general building block **13** was obtained by treatment with the amide coupling reagent. Appropriate diacylhydrazine scaffold **13** was then converted to oxadiazole compounds **6a**–**c** and **7a**–**h** by intramolecular cyclization followed by dehydration in presence of $POCl_3$.[20] The thiadiazole analog of **6a,** that is **6d,** was obtained from the intermediate **13** by treatment with Lawesson's reagent. The corresponding triazole analog **6e** was obtained from the intermediate **10a** in four steps: via formation of the corresponding N-protected amide **14** followed by thioamide **15**, and subsequently by $Hg(OAc)_2$ induced condensation of the intermediate **15** with appropriate acylhydrazine **12**, followed by deprotection of 2,4-dimethoxy benzyl group.[21–23]

In conclusion, starting from a near micromolar active high-throughput screening hit **1**, systematic structure-activity relationship study led to the identification of several potent and selective hGPR91 antagonists. Two independent series were developed, namely amides **2**–**5**, and amide-bio-isosteric analogs **6**–**7**. Initial hurdle of poor oral bioavailability, observed in series **2**–**4** and **6**, was subsequently overcome in series **5** and **7** respectively (Table 1). A new pharmacodynamic (PD) assay was set up in anesthetized Wistar rats based on succinate induced increase in mean arterial pressure. Employing two representative tool compounds **2c** and **4c**, in the PD study, GPR91 target engagement was demonstrated in vivo (Fig. 4). *To the best of our knowledge, this is the first report of the discovery and pharmacodynamic characterization of GPR91 antagonists*. The compounds presented here (e.g., **5g**, **7e**) may serve as pharmacological tools for establishing animal proof-of-concept of GPR91 modulation in several potential therapeutic indications such as: renal hypertension, diabetic nephropathy, autoimmune disease, retinal angiogenesis, and diabetic retinopathy. In addition, we hope this communication will serve as a catalyst for further studies leading to better understanding of the target and eventually to a new line of therapy. A complete medicinal chemistry and pharmacological validation of GPR91 will be disclosed elsewhere in the form of full paper.

Acknowledgments

Described work was carried out as a part of collaborative program between Advinus Therapeutics and Merck Research Laboratories. We thank all the members of much larger GPR91 team, business alliance leaders, and senior management from both the organizations. We thank Dr. Mahesh Mone for analytical support, and Dr. Anup Ranade for managing intellectual property. Advinus publication no. ADV-A-012.

Supplementary data

Supplementary data (hGPR91 antagonistic screening assay protocol; series wise hGPR91 IC_{50} along with metabolic stability data of representative compounds (*Table* S1–S4); spectral characterization of key compounds; additional information on animal studies) associated with this article can be found, in the online version, at doi:10.1016/j.bmcl.2011.04.091.

References and notes

1. He, W.; Miao, F. J.-P.; Lin, D. C.-H.; Schwandner, R. T.; Wang, Z.; Gao, J.; Chen, J.-L.; Tian, H.; Ling, L. *Nature* **2004**, *429*, 188.
2. Gonzalez, N. S.; Communi, D.; Hannedouche, S.; Boeynaems, J.-M. *Purinergic Signalling* **2004**, *1*, 17.
3. Regard, J. B.; Sato, I. T.; Coughlin, S. R. *Cell* **2008**, *135*, 561.
4. Hakak, Y.; Lehmann-Bruinsma, K.; Phillips, S.; Le, T.; Liaw, C.; Connolly, D. T.; Behan, D. P. *J. Leukoc. Biol.* **2009**, *85*, 837.
5. Sapieha, P.; Sirinyan, M.; Hamel, D.; Zaniolo, K.; Joyal, J.-S.; Cho, J.-H.; Honoré, J.-C.; Kermorvant-Duchemin, E.; Varma, D. R.; Tremblay, S.; Leduc, M.; Rihakova, L.; Hardy, P.; Klein, W. H.; Mu, X.; Mamer, O.; Lachapelle, P.; Polo, A. D.; Beauséjour, C.; Andelfinger, G.; Mitchell, G.; Sennlaub, F.; Chemtob, S. *Nature Med.* **2008**, *14*, 1067.
6. Hebert, S. C. *Nature* **2004**, *429*, 143.
7. Sadagopan, N.; Li, W.; Roberds, S. L.; Major, T.; Preston, G. M.; Yu, Y.; Tones, M. A. *Am. J. Hypertens.* **2007**, *20*, 1209.
8. (a) Toma, I.; Kang, J. J.; Sipos, A.; Vargas, S.; Bansal, E.; Hanner, F.; Meer, E.; Peti-Peterdi, J. *J. Clin. Invest.* **2008**, *118*, 2526; (b) Peti-Peterdi, J.; Kang, J. J.; Toma, I. *Nephrol. Dial. Transplant.* **2008**, *23*, 3047–3049; (c) Vargas, S. L.; Toma, I.; Kang, J. J.; Meer, E. J.; Peti-Peterdi, J. *J. Am. Soc. Nephrol.* **2009**, *20*, 1002; (d) Peti-Peterdi, J. *Kidney Int.* **2010**, *78*, 1214.
9. Correa, P. R. A. V.; Kruglov, E. A.; Thompson, M.; Leite, M. F.; Dranoff, J. A.; Nathanson, M. H. *J. Hepatol.* **2007**, *47*, 262.
10. Rubic, T.; Lametschwandtner, G.; Jost, S.; Hinteregger, S.; Kund, J.; Carballido-Perrig, N.; Schwärzler, C.; Junt, T.; Voshol, H.; Meingassner, J. G.; Mao, X.; Werner, G.; Rot, A.; Carballido, J. M. *Nature Immunol.* **2008**, *9*, 1261.
11. Kermorvant-Duchemin, E.; Sapieha, P.; Sirinyan, M.; Beauchamp, M.; Checchin, D.; Hardy, P.; Sennlaub, F.; Lachapelle, P.; Chemtob, S. *Doc. Opthalmol.* **2010**, *120*, 51.
12. We are not aware of any prior art literature of GPR91 antagonist. However, there are patent applications claiming method of screening of drug candidates modulating GPR91 and the method of treatment to various therapeutic indications. Please see, (a) Li, K.; Wang, S.-W.; Hu, G.; Yao, Z. PCT international publication no. WO 2005/010152 A2. (b) Golz, S.; Brüggemeier, U.; Geerts, A.; Summer, H. PCT international publication no. WO 2005/050220 A1. (c) Carballido Herrera, J. M.; Lametschwandtner, G.; Werner, G.; Rot, A. PCT international publication no. WO 2006/117193 A2. (d) Hakak, Y.; Liu, L.; Bruinsma, K. PCT international publication no. WO 2009/011885 A1.
13. Supplementary data referred for a brief description of GPR91 antagonist screening assay protocol used in HTS as well as for the SAR work presented here.
14. For literature on BK_1R antagonists related to **1**, please see: (a) Kuduk, S. D.; Marco, C. N. D.; Chang, R. K.; Wood, M. R.; Kim, J. J.; Schirripa, K. M.; Murphy, K. L.; Ransom, R. W.; Tang, C.; Torrent, M.; Ha, S.; Prueksaritanont, T.; Pettibone, D. J.; Bock, M. G. *Bioorg. Med. Chem. Lett.* **2006**, *16*, 2791; (b) Wood, M. R.; Kuduk, S. D.; Bock, M. G.; Chang, R. K. US Patent application publication no. US 2006/0128765 A1.; (c) Wood, M. R.; Su, D.-S.; Wai, J. M.-C. US Patent application publication no. US 2006/0173023 A1.; (d) Kuduk, S. D.; Marco, C. N. D.; Chang, R. K.; Wood, M. R.; Schirripa, K. M.; Kim, J. J.; Wai, J. M.-C.; DiPardo, R. M.; Murphy, K. L.; Ransom, R. W.; Harrell, C. M.; Reiss, D. R.; Holahan, M. A.; Cook, J.; Hess, J. F.; Sain, N.; Urban, M. O.; Tang, C.; Prueksaritanont, T.; Pettibone, D. J.; Bock, M. G. *J. Med. Chem.* **2007**, *50*, 272.
15. (a) Meissner, R. S.; Perkins, J. J.; Duong, L. T.; Hartman, G. D.; Hoffman, W. F.; Huff, J. R.; Ihle, N. C.; Leu, C. –T.; Nagy, R. M.; Naylor-Olsen, A.; Rodan, G. A.; Rodan, S. B.; Whitman, D. B.; Wesolowski, G. A.; Duggan, M. E. *Bioorg. Med. Chem. Lett.* **2002**, *12*, 25; (b) Dormer, P. G.; Eng, K. K.; Farr, R. N.; Humphrey, G. R.; McWilliams, J. C.; Reider, P. J.; Sager, J. W.; Volante, R. P. *J. Org. Chem.* **2003**, *68*, 467.
16. (a) Turner, J. A. *J. Org. Chem.* **1983**, *48*, 3401; (b) Rivera, N. R.; Hsiao, Y.; Cowen, J. A.; McWilliams, C.; Armstrong, J.; Yasuda, N.; Hughes, D. L. *Synth. Commun.* **2001**, *31*, 1573.
17. *N-[(3'-Methylbiphenyl-4-yl)methyl]-4-([1,8]naphthyridin-2-yl)butyramide*, **2c**. Mp: 140–142 °C. ^{1}H NMR (400 MHz, $CDCl_3$): δ 2.30 (quint, J = 7 Hz, 2H), 2.39 (t, J = 7 Hz, 2H), 2.41 (s, 3H), 3.14 (t, J = 7 Hz, 2H), 4.48 (d, J = 5.6 Hz, 2H), 6.42 (br t, J = 5.6 Hz, 1H, -NH-), 7.16 (d, J = 7.2 Hz, 1H), 7.32 (t, J = 7.6 Hz, 1H), 7.34–7.38 (aromatics, 4H), 7.42 (d, J = 8.4 Hz, 1H), 7.46 (dd, J = 8.2, 4.4 Hz, 1H), 7.53 (d, J = 8.4 Hz, 2H), 8.12 (d, J = 8.3 Hz, 1H), 8.17 (dd, J = 8.1 Hz, 2 Hz, 1H), 9.07 (dd, J = 4.4, 2 Hz, 1H). ^{13}C NMR (100 MHz, DMSO-D_6): δ 21.08, 24.86, 34.86, 37.76, 41.72, 120.90, 121.62, 122.55, 123.64, 126.53 (2C), 127.16, 127.74 (2C), 127.90, 128.75, 137.26, 137.61, 137.97, 138.71, 138.83, 139.90, 153.16, 155.29, 165.47, 171.80. HPLC purity: 99.6%. MS (m/z): 396.0 [M+1] base peak. HRMS (m/z): Calcd For [M+1]: 396.2075; Found: 396.2094.
18. *N-[(S)-1-(4'-Fluoro-3'-trifluoromethylbiphenyl-4-yl)ethyl]-2-[4-([1,8]naphthyridin-2-yl)phenyl]acetamide*, **4c**. Mp: 198–200 °C. ^{1}H NMR (400 MHz, DMSO-D_6): δ 1.42 (d, J = 6.9 Hz, 3H), 3.59 (s, 2H), 4.98 (quintet, J = 7.1 Hz, 1H), 7.43 (d, J = 8.2 Hz, 2H), 7.48 (d, J = 8.2 Hz, 2H), 7.56–7.65 (aromatics, 2H), 7.69 (d, J = 8.2 Hz, 2H), 7.96 (br d, J = 6 Hz, 1H), 8.00–8.05 (aromatics, 1H), 8.27 (d, J = 8.4 Hz, 3H), 8.48 (dd, J = 8.0, 1.8 Hz, 1H), 8.56 (d, J = 8.6 Hz, 1H), 8.70 (d, J = 7.9 Hz, 1H), 9.09 (dd, J = 4.0, 1.8 Hz, 1H). ^{13}C NMR

(100 MHz, DMSO-D_6): δ 22.52, 42.16, 47.81, 116.60–117.40 (m, –CF_3), 117.74 (J = 20 Hz), 119.49, 121.28, 121.60, 122.06, 123.99, 125.05 (d, J = 3.9 Hz), 126.67 (2C), 126.95 (2C), 127.43 (2C), 129.62 (2C), 133.28 (d, J = 8.5 Hz), 136.09, 136.41, 137.05 (d, J = 3 Hz), 137.28, 138.71 (J = 7.4 Hz), 144.79, 153.93, 155.49, 158.31 (d, J = 252 Hz), 158.91, 168.96. HPLC purity: 99.1%. Chiral purity: 100% (chiral HPLC). MS (m/z): 530.0 [M+1] base peak. HRMS (m/z): Calcd for [M+1]: 530.1855; Found: 530.1854. $[\alpha]_D$ = +127.15 (25 °C, c 0.3, $CHCl_3$).

19. *N-[{3-(3-trifluoromethyl-4-fluorophenyl)isoxazol-5-yl}methyl]-4-([1,8]naphthyridin-2-yl)butyramide*, **5g**. Mp: 168–170 °C. ^{1}H NMR (400 MHz, DMSO-D_6): δ 2.04 (quintet, J = 7.4 Hz, 2H), 2.23 (t, J = 7.4 Hz, 2 H), 2.95 (t, J = 7.5 Hz, 2H), 4.43 (d, J = 5.7 Hz, 2H), 7.11 (s, 1H), 7.52 (d, J = 8.4 Hz, 1H), 7.54 (dd, J = 8.1, 4.4 Hz, 1H), 7.64 (t, J = 9.5 Hz, 1H), 8.19 (d, J = 7.0 Hz, 1H), 8.22–8.28 (m, 1H), 8.34 (d, J = 8.4 Hz, 1H), 8.39 (dd, J = 8.1, 1.9 Hz, 1H), 8.56 (br t, J = 5.7 Hz, –NH–), 8.99 (dd, J = 4.4, 1.9 Hz, 1H). ^{13}C NMR (100 MHz, DMSO-D_6): δ 24.61, 34.47, 34.66, 37.61, 100.23, 117.0–118.0 (m, CF_3), 118.24 (J = 21 Hz), 120.96, 121.72, 122.57, 123.80, 125.42-125.48 (m), 125.80 (d, J = 3.1 Hz), 133.54 (d, J = 9.3 Hz), 137.34, 137.72, 153.23, 155.32, 159.7 (J = 256 Hz), 160.07, 165.47, 172.12, 172.21. HPLC purity: 99.33%. MS (m/z): 459.3 [M+1] base peak. HRMS (m/z): Calcd for [M+1]: 459.1444; Found: 459.1459.
20. For oxadiazole synthesis, see: (a) Cao, S.; Qian, X.; Song, G.; Huang, Q. *J. Fluorine Chem.* **2002**, *117*, 63; (b) Chang, E.-M.; Lin, C.-J.; Wong, F. F.; Yeh, M.-Y. *Heterocycles* **2006**, *68*, 733.
21. For 1,2,4-triazole synthesis, see: Boeglin, D.; Cantel, S.; Heitz, A.; Martinez, J.; Fehrentz, J.-A. *Org. Lett.* **2003**, *5*, 4465.
22. *2-{3-[5-(3'-Chlorobiphenyl-4-yl)-[1,3,4]oxadiazol-2-yl]propyl}[1,8]naphthyridine* **6a**. Mp: 162–164 °C. ^{1}H NMR (DMSO-D_6): δ 2.33 (quint, J = 7.3 Hz, 2H), 3.06 (t, J = 7.4 Hz, 2H), 3.12 (t, J = 7.3 Hz, 2H), 7.47 (dt, J = 7.7, 1.6 Hz, 1H), 7.51 (t, J = 7.7 Hz, 1H), 7.54 (d, J = 8.5 Hz, 1H), 7.55 (d, J = 8.6 Hz, 1H), 7.71 (dt, J = 7.5, 1.6 Hz, 1H), 7.80 (t, J = 1.6 Hz, 1H), 7.89 (d, J = 8.5 Hz, 2H), 7.99 (d, J = 8.5 Hz, 2H), 8.34 (d, J = 8.3 Hz, 1H), 8.37 (dd, J = 8.2, 2.0 Hz, 1H), 8.99 (dd, J = 4.2, 2.0 Hz, 1H). ^{13}C NMR (DMSO-D_6): δ 24.36, 25.05, 37.17, 120.97, 121.72, 122.70, 123.01, 125.59, 126.61, 127.02 (2C), 127.75 (2C), 128.14, 130.97, 133.94, 137.29, 137.72, 140.95, 141.47, 153.25, 155.29, 163.61, 164.84, 166.73. MS (m/z): 427.0 [M (^{35}Cl) +1] base peak. HPLC purity: 99%.
23. *2-{4-[5-(3-Chloro-4-trifluoromethoxyphenyl)-[1,3,4]oxadiazol-2-yl]butyl}-[1,8]naphthyridine*, **7e**. Mp: 80–82 °C. ^{1}H NMR (400 MHz, $CDCl_3$): δ 1.98 (quint, J = 7.5 Hz, 2H), 2.08 (quint, J = 7.5 Hz, 2H), 3.00 (t, J = 7.4 Hz, 2H), 3.12 (t, J = 7.4 Hz, 2H), 7.38 (d, J = 8.2 Hz, 1H), 7.42-7.48 (aromatics, 2H), 7.96 (dd, J = 8.2, 1.9 Hz, 1H), 8.10 (d, J = 8.4 Hz, 1H), 8.13 (d, J = 1.8 Hz, 1H), 8.15 (dd, J = 8.0, 1.7 Hz, 1H), 9.07 (dd, J = 4.0, 1.7 Hz, 1H). ^{13}C NMR (100 MHz, DMSO-D_6): δ 33.96, 34.89, 37.30, 47.14, 129.42 (J = 258 Hz, –CF_3), 130.39, 131.13, 132.05, 133.34, 133.68, 136.50, 136.69, 138.19, 146.77, 147.13, 155.48, 162.68, 164.80, 171.46, 175.04, 176.94. HPLC purity: 99.27%. MS (m/z): 448.9 [M(^{35}Cl) +1] base peak.